*Short Communication*

# Preparation and Electrochemical Performance of a Honeycomb-like Porous Anode Material

*Xin-xiu Li[1], Jiao Hou[2], Xing-wei Wang[2], Xiong-fei Liu[1], and Chun-ping Hou[2,\*]*

[1] China University of Mining and Technology Yinchuan College, Yinchuan Ningxia 750021, P.R. China
[2] Ningxia BOLT Technologies Co., Ltd., Yinchuan Ningxia, 750002, P.R. China
[*]E-mail: hcp400@163.com

Ground coffee is used to prepare a honeycomb-like porous anode material for Li-ion batteries. The microstructure and morphology of the as-prepared samples are characterized by X-ray diffraction and scanning electron microscopy. The material has a honeycomb-like porous morphology, a smaller specific surface area than graphitized coke, and a relatively low degree of graphitization. Electrochemical tests show as-prepared anode material to have good low-temperature performance, large rate capability, and good cycling performance. At -30 °C, the material delivers a discharge capacity of 52.1 mAh $g^{-1}$, which is more than three times that of graphitized needle coke artificial graphite anode material that is commercially available. Thus, it is suitable for high-power or energy storage batteries.

## 1. INTRODUCTION

Lithium ion batteries (LIBs) have many advantages, and have been used in many types of electronics [1-4]. Recently, much effort has been devoted to expanding their practical use in high-power and long-cycle applications, such as electric vehicles and dispersed energy storage, which require LIBs to have an excellent life span, and be reliable and safe [5, 6]. Graphite is the most widely used anode material due to its flat charge/discharge profiles, giving it a theoretical specific capacity of 372 mAh $g^{-1}$ [7].

However, at low temperatures, graphite anodes suffer from severe limitations in rate capability and cycling, and produce an abrupt decrease in the Li intercalation capacity at temperatures below -20 °C. At -30 °C, graphite completely loses its intercalation ability [8-10]. At low temperatures, graphite

anodes suffer from high polarization that occurs during Li loading, a reduced $Li^+$ ion solid-state diffusivity, as well as to an increase in the ohmic resistance of the active material. Materials including mesophase carbon micro beads [11], hard carbon [12, 13], soft carbon [14], and metallic oxides [15, 16] for high-performance anodes have been the focus of research, and have overcome the limitations of graphite anodes. In addition, many porous structure designs have been used to improve greatly the electrochemical performance of the electrode materials owing to their many pores and large specific surface area, which keep active anode materials in full contact with the electrolyte and facilitate $Li^+$ intercalation/deintercalation [17-22]. Tian et al [23] synthesized porous carbon anode material with coffee grounds by an easy carbonization and activation approach, which obtained a specific surface area of 352 $m^2$ $g^{-1}$.

In this study, a honeycomb-like porous (HP) anode material was synthesized from ground coffee by a facile method and showed much better electrochemical performances compared with a graphitized needle coke artificial graphite (CAG) anode material that is commercially available.

## 2. EXPERIMENTAL

Ground coffee was carbonized at 350 °C for 4 h in a pure $N_2$ atmosphere to obtain the precursor. This was ground to 200 mesh and coated uniformly with 8wt % high-temperature petroleum asphalt. The coated precursor was carbonized at 900 °C for 7 h in a pure $N_2$ atmosphere to obtain the target sample. A CAG sample with a diameter of approximately 16 μm and a carbon content of 99.98 wt% was supplied by Ningxia BOLT Technologies Co., Ltd. and used for comparison.

The structure of the synthesized materials was characterized by an X-ray diffraction (XRD; XRD-7000S, Shimadzu, Japan) using Cu Kα radiation (λ=0.15423 nm). The surface morphologies of the samples were observed by scanning electron microscopy (SEM; JSM-6700F, JEOL, Japan). The specific surface area was characterized with a surface area analyser (NOVA 4000e, Quantachrome, USA).

The electrochemical properties of the samples were characterised by first assembling CR2025 coin cells. The composite electrodes were prepared by mixing HP or the comparison sample (CAG) with carbon black and polyvinylidene fluoride (PVDF) in a weight ratio of 92:3:5 in N-methylpyrrolidone (NMP) solvent to form a homogeneous slurry. Then, the mixtures were coated on a copper foil and punched to disks. After drying under ambient conditions, the disks were further dried in a vacuum oven at 120 °C for 12 h. Finally, the cells were assembled in an Ar-filled glove box (LABSTAR 1250/750, MBRAUN) using lithium foil as the counter and reference electrode, a polypropylene micro-porous film (Cellgard2400) as the separator, and 1 M $LiPF_6$ in ethylene carbonate (EC), dimethyl carbonate (DMC) and diethyl carbonate (DEC) (1:1:1, v/v/v) (GuangzhouTinci) as the electrolyte. A LAND batteries testing system (LAND CT2001A, Wuhan Jinnuo, China) was used to perform the galvanostatic charge/discharge tests in the potential range of 0.03-2.0 V (vs.$Li^+$/Li) at a rate of 0.1 C, 0.5 C and 1C (where 1 C = 372 mA $g^{-1}$).

## 3. RESULTS AND DISCUSSION
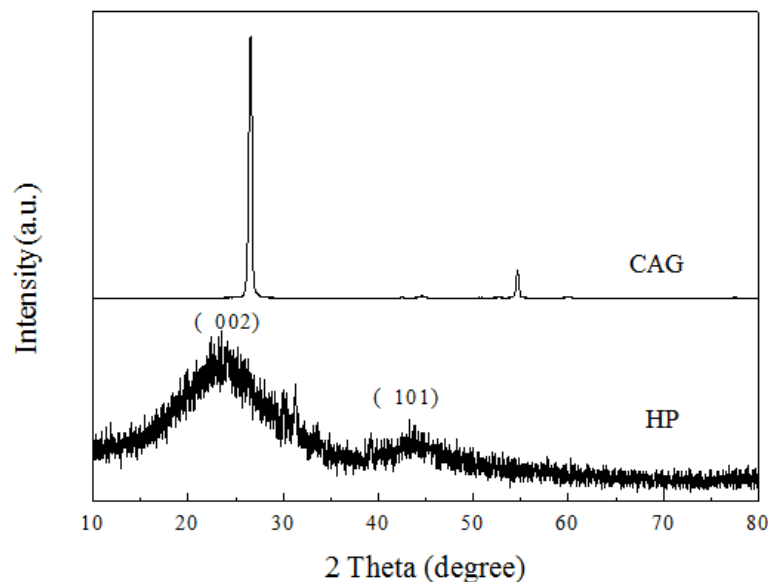


**Figure 1.** XRD patterns of HP and CAG.

The XRD patterns of HP and CAG are shown in Fig. 1. In contrast to the perfect graphite crystal structure of CAG, the characteristic features of the as-prepared HP sample were typical of poorly organized carbon with a very low degree of graphitization. The XRD diffractogram for the as-prepared samples contained clear diffraction peaks at 2θ of 23°-25° and 42°-44°, which corresponded to the (002) and (101) plane signals of hard carbon, respectively [12, 24]. Compared with diffraction peaks at 26.4° and 44.5° of CAG, the shift to a lower 2θ indicated that HP had a larger interlamellar spacing that allowed Li$^+$ to diffuse more easily.
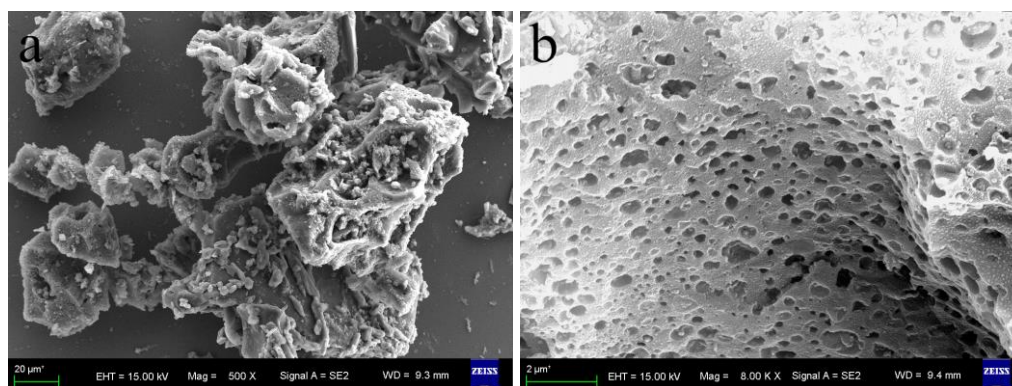


**Figure 2.** SEM images of the HP samples carbonized at (a) 350 and (b) 900 °C.

Fig. 2 presents SEM images of the HP samples carbonized at 350 and 900 °C. The honeycomb-like porous structure appeared after carbonization at 900 °C, and no obvious porous structure was produced at 350 °C. As the temperature and reaction time increases, the gases are released from the

material, creating many micro- and nano-pores. Although the as-prepared sample had a honeycomb-like porous structure, it also had a small specific surface area of 2.512 m$^2$ g$^{-1}$, which is different from previous studies [17, 24-26]. The specific surface area of anode materials for LIBs is too high to be used in practical application.
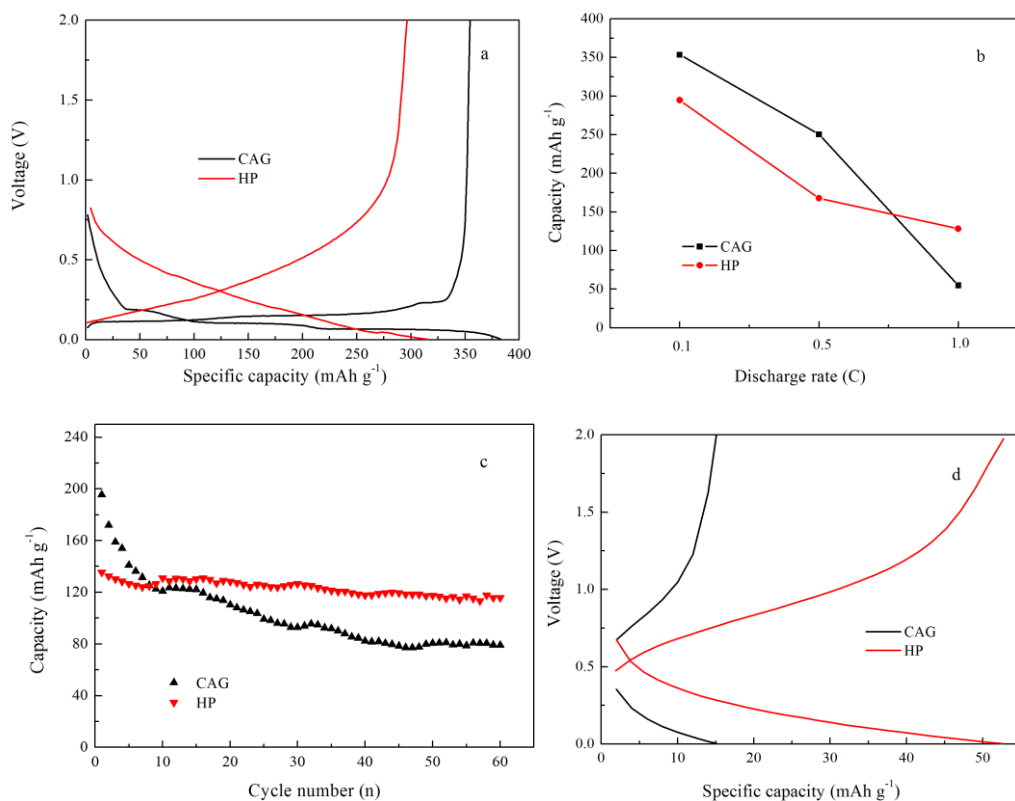


**Figure 3.** Electrochemical performance of HP and CAG. (a) Charge and discharge curves at a rate of 0.1C at room temperature, (b) rate capabilities at room temperature, (c) cycle performances at a rate of 0.5C at room temperature, and (d) charge and discharge curves at -30 °C.

The charge-discharge curves of HP and CAG at a rate of 0.1C at room temperature are shown in Fig. 3 (a). HP exhibited a lower discharge capacity than CAG (296.3 vs. 354.4 mAh g$^{-1}$). However, its charge/discharge plateaus were much higher than those of CAG, and these special characteristics would suppress Li plating during electrochemical Li$^+$ intercalation and de-intercalation, improving the safety of an LIB.

Fig. 3 (b) shows the rate capabilities of HP and CAG at rates of 0.1, 0.5, and 1.0 C at room temperature. Although HP delivered a lower discharge capacity of 296.3 mAh g$^{-1}$ at a rate of 0.1 C, its discharge ability increased as the discharge rate increased. For discharge at a rate of 1.0 C, HP delivered a much higher discharge capacity of 129.1 mAh g$^{-1}$, which was more than twice that of CAG. It also exhibited better cycling performance, with a capacity retention of 85.45% at a rate of 0.5 C at room temperature after 60 cycles, whereas CAG only had a capacity retention of 40.4% (as shown in Fig. 3 (c)).

Shown in Fig. 3 (d), good low-temperature performance of an anode material is necessary for electric vehicles and dispersed energy storage. At -30 °C, HP delivered a discharge capacity of 52.1 mAh g$^{-1}$, which was more than three times that of CAG, and exhibited excellent low-temperature performance. The discharge capacities of CAG with similar anode materials that were described in literatures at low temperature are also listed in Table 1. The above-mentioned discharge capacity is far beyond the results in previous literatures about untreated graphite anode. Nobili et al. [9] reported that graphite without Sn coating delivered almost no capacity at -30 °C. Markevich et al. [10] found that at -30 °C only 3.6% (13 mAh g$^{-1}$) of Li was extracted from the fully charged graphite anode. Yaqub et al. [27] revealed that pitch coated graphite electrode delivered a discharge capacity of 1.40 mAh g$^{-1}$ with high loading at -32 °C which caused by abrupt decrease of Li-ion diffusion. The $D_{Li+}$ of graphite electrode with low loading downgraded from $1.38 \times 10^{-8}$ cm$^2$ s$^{-1}$ at room temperature to $4.79 \times 10^{-13}$ cm$^2$ s$^{-1}$ at -32 °C. The improvement in electrochemical performance, including rate capability, cycle stability, and low-temperature characteristics, were attributed to the larger interlamellar spacing and honeycomb-like porous structure of HP. The larger the interlamellar spacing, the more easily Li$^+$ diffuses and intercalates/de-intercalates in the HP anode material. Moreover, the honeycomb-like porous microstructure has various advantages, such as short solid-state diffusion lengths and more diffusion passageways for Li$^+$, full contact with the electrolyte for the active material, reasonable electrical conductivity of the porous carbon due to a well-interconnected wall structure, and a large number of active sites for charge-transfer reactions, which are important factors in improving the electrochemical performance of HP anode material [17, 25, 28].

**Table 1.** The discharge capacities of CAG with similar anode materials that were described in literatures at low temperature.

| Sample | Discharge capacity (mAh g$^{-1}$) | Temperature (°C) | Ref. |
|--------|-----------------------------------|------------------|------|
| NG | 1 | -30 | [9] |
| Sn-graphite | 94 | -30 | [9] |
| NG | 13 | -30 | [10] |
| C-graphite | 1.4 | -32 | [27] |
| CAG | 15 | -30 | This work |
| HP | 52.1 | -30 | This work |

## 4. CONCLUSIONS

An HP anode material was prepared by a facile method from ground coffee. The sample had a honeycomb-like porous morphology, a smaller specific surface area of 2.512 m$^2$ g$^{-1}$ compared with CAG, a relatively low degree of graphitization. The HP anode material showed much better

electrochemical performance than CAG, especially at low temperatures. Thus, HP is a potential anode material for powerful LIBs, and is suitable for high-power applications or energy storage.

**References**

1. J.R. Szczech and S. Jin, *Energy Environ. Sci.*, 4 (2011) 56.
2. S.-M. Oh, S.-T. Myung, J.B. Park, B. Scrosati, K. Amine, and Y.-K. Sun, *Angew. Chem. Int. Edit.*, 51 (2012) 1853.
3. J.K. Kim and A. Manthiram, *Nature*, 390 (1997) 265.
4. J.M. Tarascon and M. Armand, *Nature*, 414 (2001) 359.
5. K. Amine, I. Belharouak, Z. Chen, T. Tran, H. Yumoto, N. Ota, S.-T. Myung, and Y.-K. Sun, *Adv. Mater.*, 22 (2010) 3052.
6. J.-J. Chen, M.D. Symes, S.-C. Fan, M.-S. Zheng, H.N. Miras, Q.-F. Dong, and L. Cronin, *Adv. Mater.*, 27 (2015) 4649.
7. a. Naji, P. Willmann, and D. Billaud, *Carbon*, 36 (1998) 1347.
8. G. Park, N. Gunawardhana, H. Nakamura, Y.-S. Lee, and M. Yoshio, *J. Power Sources*, 199 (2012) 293.
9. F. Nobili, M. Mancini, S. Dsoke, R. Tossici, and R. Marassi, *J. Power Sources*, 195 (2010) 7090.
10. E. Markevich, G. Salitra, and D. Aurbach, *J Electrochem. Soc.*, 163 (2016) A2407.
11. H. Wang, T. Abe, S. Maruyama, Y. Iriyama, Z. Ogumi, and K. Yoshikawa, *Adv. Mater.*, 17 (2005) 2857.
12. X. Zhang, C. Fan, L. Li, W. Zhang, W. Zeng, X. He, and S. Han, *Electrochim. Acta*, 149 (2014) 94.
13. J. Ni, Y. Huang, and L. Gao, *J. Power Sources*, 223 (2013) 306.
14. C. Ma, Y. Zhao, J. Li, Y. Song, J. Shi, Q. Guo, and L. Liu, *Carbon*, 64 (2013) 553.
15. Y. Ma, C. Fang, B. Ding, G. Ji, and J.Y. Lee, *Adv. Mater.*, 25 (2013) 4646.
16. Y. Ren, J. Zhang, Y. Liu, H. Li, H. Wei, B. Li, and X. Wang, *ACS Appl. Mater. Inter.*, 4 (2012) 4776.
17. K.T. Lee, J.C. Lytle, N.S. Ergang, S.M. Oh, and A. Stein, *Ad. Funct. Mater.*, 15 (2005) 547.
18. Z. Zhang, Y. Wang, W. Ren, Q. Tan, Y. Chen, H. Li, Z. Zhong, and F. Su, *Angew. Chem. Int. Edit.*, 53 (2014) 5165.
19. L. Zhang, J. Deng, L. Liu, W. Si, S. Oswald, L. Xi, M. Kundu, G. Ma, T. Gemming, S. Baunack, F. Ding, C. Yan, and O.G. Schmidt, *Adv. Mater.*, 26 (2014) 4527.
20. F. Wang, R. Song, H. Song, X. Chen, and J. Zhou, *Carbon*, 81 (2014) 314.
21. D. Chen, X. Mei, G. Ji, M. Lu, J. Xie, J. Lu, and J.Y. Lee, *Angew. Chem. Int. Edit.*, 51 (2012) 2409.
22. Y.-K. Sun, S.-M. Oh, H.-K. Park, and B. Scrosati, *Adv. Mater.*, 23 (2011) 5050.
23. W. Tian, X. Wu, and X. Wei, *Journal of Jilin University (Science Edition)*, 52 (2014) 802.
24. H.-g. Wang, Y. Wang, Y. Li, Y. Wan, and Q. Duan, *Carbon*, 82 (2015) 116.
25. F. Wang, R. Song, H. Song, X. Chen, J. Zhou, Z. Ma, M. Li, and Q. Lei, *Carbon*, 81 (2015) 314.
26. Y. Su, Y. Liu, P. Liu, D. Wu, X. Zhuang, F. Zhang, and X. Feng, *Angew. Chem. Int. Edit.*, 54 (2015) 1812.

27.    A. Yaqub, Y.-J. Lee, M.J. Hwang, S.A. Pervez, U. Farooq, J.-H. Choi, D. Kim, H.-Y. Choi, S.-B. Cho, and C.-h. Doh, *J. Mater. Sci*, 49 (2014) 7707.
28.    K.-X. Wang, X.-H. Li, and J.-S. Chen, *Adv. Mater.*, 27 (2015) 527.